A Free Energy Model for Piezoceramic Materials

Ralph C. Smith*, Stefan Seelecke† and Zoubeida Ounaies‡

*Center for Research in Scientific Computation, North Carolina State Univ., Raleigh, NC 27695
†Mechanical and Aerospace Engineering, North Carolina State University, Raleigh, NC 27695
‡Mechanical Engineering, Virginia Commonwealth University Richmond VA 23284-3015

Abstract

This paper addresses the development of a free energy model for quantifying the hysteresis and constitutive nonlinearities inherent to piezoceramic materials. In the first step of the development, free energy relations for a single crystal with uniform lattice are considered and used to construct evolution equations which quantify the polarization as a function of the applied field. The effects of nonuniform lattice structures, nonhomogeneous effective fields and polycrystalline materials are then incorporated through the use of appropriate distributions in the free energy formulation. The resulting model, which is an extension of the Müller-Achenbach-Seelecke theory for shape memory alloys, is low-order and hence highly efficient to implement. Attributes of the model are illustrated through comparison with experimental data.

Keywords: Free energy model, hysteresis, constitutive nonlinearities, piezoceramic materials

1. Introduction

An inherent property of piezoelectric materials is the presence of hysteresis and constitutive nonlinearities in the relation between the applied field and resulting polarization. For a number of applications, the deleterious effects due to the hysteresis and nonlinearities can be mitigated through feedback mechanisms; this has led to the successful use of piezoceramic transducers in regimes ranging from structural acoustic control to hybrid motor design. However, in other regimes, noise to signal ratios preclude a complete dependence on feedback laws to attenuate hysteresis which necessitates alternative control designs such as model-based feedforward loops. For example, the positioning mechanisms in atomic force microscopes and nanopositioners are comprised of stacked or cylindrical PZT actuators. At low frequencies, feedback laws can attenuate the measured hysteresis, thus leading to the phenomenal success of the devices. However, at the higher frequencies required for product diagnostics or real-time monitoring of biological processes, the efficacy of feedback laws is diminished by inherent thermal and measurement noise. One means of circumventing this limitation is through the development of feedforward loops utilizing highly accurate and efficient constitutive models. In this paper, we develop such a model through the combination of free energy principles and probabilistic distributions to accommodate material and field nonhomogeneities.

To provide a context for this approach, we note that current hysteresis models can roughly be categorized as microscopic, macroscopic or semi-macroscopic (mesoscopic) in nature. Microscopic theories are typically developed at the grain or lattice level and hence require a substantial number of parameters and states [7]; hence they are difficult to employ for system design or control. Macroscopic models lie at the opposite end of the spectrum and are typically based on phenomenological or empirical principles [2, 3, 9]. They are typically low-order but often have nonphysical parameters which makes them difficult to update to accommodate changing

*Email: rsmith@eos.ncsu.edu; Telephone: 919-515-7552
†Email: stefan_seelecke@ncsu.edu; Telephone: 919-515-5282
‡Email: zounaies@vcu.edu; Telephone: (804) 827-7025

operating conditions. The lack of a physical basis for many macroscopic models also makes it difficult to incorporate frequency, temperature or load dependencies required for broadband transduction or slowly changing operating conditions. Semi-macroscopic models are based on energy principles but employ macroscopic averages to obtain effective parameters [1, 4, 11, 13]. Hence they are low-order but incorporate, to varying degrees, the physical principles which produce the phenomena being modeled. The model presented here is semi-macroscopic in nature.

In the first step of the development, Helmholtz and Gibbs free energy relations are constructed for materials having uniform lattices, and evolution equations which quantify the polarization resulting from an applied field are developed. This yields a model for homogeneous single crystals. The effects of nonuniform lattices, variations in effective fields, and polycrystalline materials are then incorporated through the use of appropriate distributions in the free energy formulations. The resulting model, which is an extension of the Müller-Achenbach-Seelecke theory for shape memory compounds [8, 10], is low-order and hence highly efficient to implement. Because of its energy basis, a number of the parameters are physical which facilitates initial construction of the model and updating to accommodate slow deviations in operating conditions. Finally, as illustrated in [14, 15], the model enforces the wiping out property and closure of both symmetric and asymmetric minor loops.

The quintessential free energy relations are developed in Section 2 for a single crystal and extended in Section 3 to provide a macroscopic model for polycrystalline compounds with variations in effective field. The accuracy of the model is illustrated in Section 4 through comparison with data from a PZT5A wafer.

2. Free Energy Model for Homogeneous Lattice

Currently employed PZT compositions are comprised of $PbTi_{1-x}O_3$ and $PbZr_xO_3$ with x chosen to optimize electromechanical coupling. To simplify this discussion, we focus on $PbTi_{1-x}O_3$ and refer the reader to [6] for discussion regarding more general PZT properties.

At temperatures below the Curie point, the material distorts from a cubic to a tetragonal form through the biasing of Ti^{4+} ions toward O^{2-} pairs. In the absence of an applied field, the equilibrium positions of the Ti^{4+} ions are determined by computing minima of the Helmholtz free energy depicted in Figure 1. As indicated in Figure 2, the application of an electric field distorts the energy landscape and a dipole switch occurs when the value of the original minimum exceeds the unstable equilibrium due to the central O^{2-} pair. At the macroscopic scale, this produces a discontinuous jump in the polarization as experimentally illustrated for single crystal Barium Titanate on pages 72-76 of [5].

The initial step in the development of the free energy model is the quantification of the free energy functional depicted in Figure 2a and hysteresis kernel depicted in Figure 2b. We initially consider a uniform lattice of volume V with N cells, each of which is assumed to have spin ± 1 and dipole moment p_0.

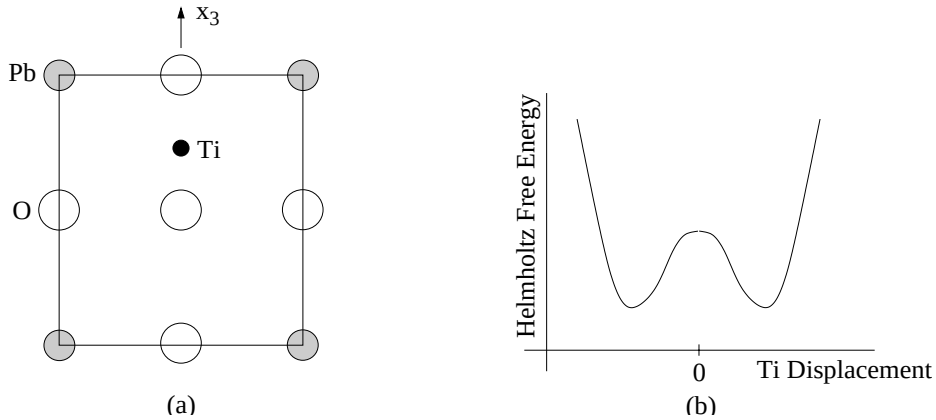

Figure 1. (a) Polar form of $PbTiO_3$; (b) Potential energy as a function of Ti position along the x_3 axis.

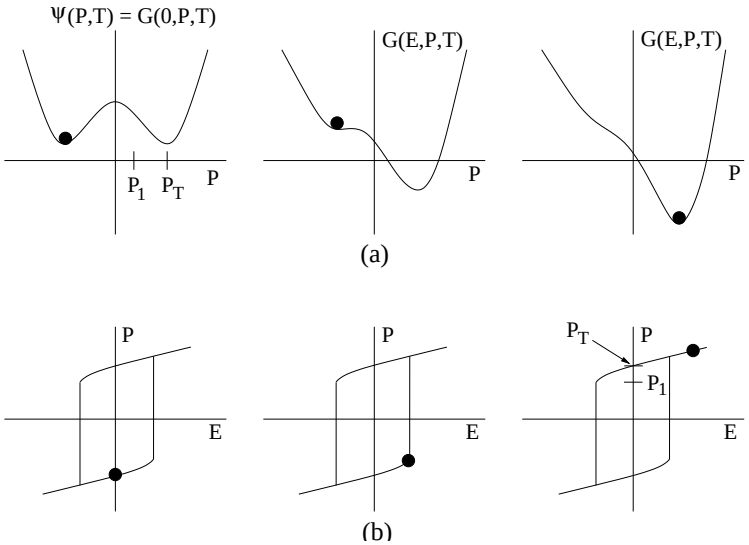

Figure 2. (a) Helmholtz energy ψ and Gibbs energy G for increasing field E; (b) Polarization P as a function of E for a single crystal with uniform lattice.

We first consider techniques for constructing the Helmholtz free energy ψ depicted in Figure 1b and Figure 2a, which incorporates the internal energy and entropic effects but neglects the electrostatic energy. As detailed in [15] and summarized in [12], a representation for ψ resulting from statistical mechanics principles is

$$\psi(P,T) = \frac{\Phi_0 N}{4V}[1-(P/P_s)^2] + \frac{TkN}{2VP_s}\left[P\ln\left(\frac{P+P_s}{P_s-P}\right) + P_s\ln(1-(P/P_s)^2)\right]. \tag{1}$$

Here P denotes the polarization, Φ_0 is the energy required to convert the spin at a single site, and $P_s = Np_0/V$ is the saturation polarization. The first term on the right hand side of (1) quantifies the internal energy for short range interactions while the second term incorporates entropic contributions at temperature T.

The free energy relation (1) provides the requisite double well behavior illustrated in Figure 1b as well as the transition to the paraelectric phase observed at temperatures above the Curie temperature T_c. However, the logarithmic nature of the entropic term reduces the efficiency of algorithms which employ this relation and makes it difficult to correlate parameters in the model with physically measured attributes of the data.

A second technique for constructing the free energy, which addresses these difficulties, is motivated by the quadratic polarization dependence noted in (1) for fixed temperatures. In this case, we consider the relation

$$\psi(P) = \begin{cases} \frac{1}{2}E_1(P+P_T)^2 & , \ P \le -P_1 \\ \frac{1}{2}E_1(P-P_T)^2 & , \ P \ge P_1 \\ \frac{1}{2}E_1(P_1-P_T)\left(\frac{P^2}{P_1}-P_T\right) & , |P| < P_1 \end{cases} \tag{2}$$

for the Helmholtz free energy. As will be established in subsequent discussion, E_1 is the reciprocal of the slope of the E-P curve, P_T is the positive intercept, and P_1 denotes the transition polarization as depicted in Figure 2.

For either of the Helmholtz relations (1) or (2), the Gibbs free energy is taken to be

$$G = \psi - EP. \tag{3}$$

From the equilibrium condition

$$\frac{\partial G}{\partial P} = 0,$$

it follows that $E = \frac{\partial \psi}{\partial P}$. Hence, the use of the relation (2) predicts a linear relation between the field and polarization after dipole switching whereas from $\frac{\partial E}{\partial P} = \frac{\partial^2 \psi}{\partial P^2}$, it follows that the slope in the hysteresis kernel is $\frac{1}{E_1}$.

The fraction of dipoles having positive and negative orientations are respectively denoted by x_+ and x_-, and the expected values of the polarization due to positively and negatively oriented dipoles are denoted by $\langle P_+ \rangle$ and $\langle P_- \rangle$. The average polarization resulting from an applied field is then

$$\overline{P} = x_+ \langle P_+ \rangle + x_- \langle P_- \rangle \ . \tag{4}$$

To establish the dependence of the expected polarization values on the field, we note that from Boltzmann principles, the probability of attaining an energy level G is given by

$$\mu(G) = Ce^{-G/kT}$$

where C is chosen to yield a total probability of 1 when integrated over all inputs and k is Boltzmann's constant. For the Gibbs energy G resulting from either of the choices (1) or (2) for ψ, the expected polarization due to positively oriented dipoles is

$$\begin{aligned} \langle P_+ \rangle &= \int_{P_0}^{\infty} P\mu(G)dP \\ &= \frac{\displaystyle\int_{P_0}^{\infty} Pe^{-G(E,P,T)V/kT}dP}{\displaystyle\int_{P_0}^{\infty} e^{-G(E,P,T)V/kT}dP} . \end{aligned} \tag{5}$$

The point P_0 is the critical point at which $\frac{\partial G}{\partial P} = 0$. Similarly, $\langle P_- \rangle$ is specified by

$$\langle P_- \rangle = \frac{\displaystyle\int_{-\infty}^{P_0} Pe^{-G(E,P,T)V/kT}dP}{\displaystyle\int_{-\infty}^{P_0} e^{-G(E,P,T)V/kT}dP} . \tag{6}$$

We note that when implementing the model, we typically replace P_0 by the inflection points P_1 and $-P_1$, respectively, in the relations (5) and (6). This simplifies the approximation of the integrals and can be motivated by observing that if one considers the forces $\frac{\partial G}{\partial P}$ due to the applied field, maximum forces occur at P_1 and $-P_1$ and hence they provide unstable equilibria. Furthermore, for materials with low thermal activation, the points P_0 and $-P_1$ essentially coincide for positive fields while P_1 and P_0 coincide for negative fields.

The dipole fractions N_+ and N_- are quantified by the differential equations

$$\begin{aligned} \dot{x}_+ &= -p_{+-}x_+ + p_{-+}x_- \\ \dot{x}_- &= -p_{-+}x_- + p_{+-}x_+ \end{aligned}$$

which can be simplified to

$$\dot{x}_+ = -p_{+-}x_+ + p_{-+}(1 - x_+) \tag{7}$$

through the identity $x_+ + x_- = 1$. Here p_{+-} denotes the likelihood of switching from positive to negative orientation while p_{-+} denotes the likelihood of switching from negative to positive (we avoid defining p_{+-} and p_{-+} as probabilities since they can be unbounded). Both are computed by specifying the probability of achieving the energy required for a jump multiplied by the frequency at which jumps are attempted. This yields the relations

$$\begin{aligned} p_{+-} &= \sqrt{\frac{kT}{2\pi m}} \frac{e^{-G(E,P_1(T),T)V/kT}}{\displaystyle\int_{P_1}^{\infty} e^{-G(E,P,T)V/kT}dP} \\ p_{-+} &= \sqrt{\frac{kT}{2\pi m}} \frac{e^{-G(E,-P_1(T),T)V/kT}}{\displaystyle\int_{-\infty}^{P_1} e^{-G(E,P,T)V/kT}dP} . \end{aligned} \tag{8}$$

Here m is the mass of the lattice volume. The polarization for a single crystal comprised of a uniform lattice is then specified by (4) with $\langle P_+ \rangle$ and $\langle P_- \rangle$ given by (5) and (6) and the dipole fractions specified as solutions to (7).

3. Polycrystalline Materials with Variable Effective Fields

The relation (4) was derived under the assumption of uniform lattice spacing in a single crystal. In the limiting case of low thermal activation, the model will thus predict the polarization relations depicted in Figure 2 since the switch from one well to the other is nearly instantaneous. Hence while the model can accurately quantify single crystal behavior of the type experimentally measured in $BaTiO_3$ (see page 76 of [5]), it does not accurately predict the more gradual transition through the remanent polarization measured in polycrystalline PZT. In this section, we incorporate the effects of nonuniform lattice configurations, polycrystallinity and variable effective fields to provide a model which accurately characterizes hysteresis in PZT and ensures minor loop closure.

As illustrated in Figure 3, nonuniformities in the lattice produce a distribution of Helmholtz and Gibbs free energies which are manifested as variations in the width of the hysteresis kernel predicted by (4). Similar variations are produced in polycrystalline materials.

For the Helmholtz model (2), the variability in the lattice structure can be incorporated by considering P_T, P_1 or $\widetilde{E}_1 = E(P_T - P_1)$ to be manifestations of an underlying distribution rather than fixed values as assumed for

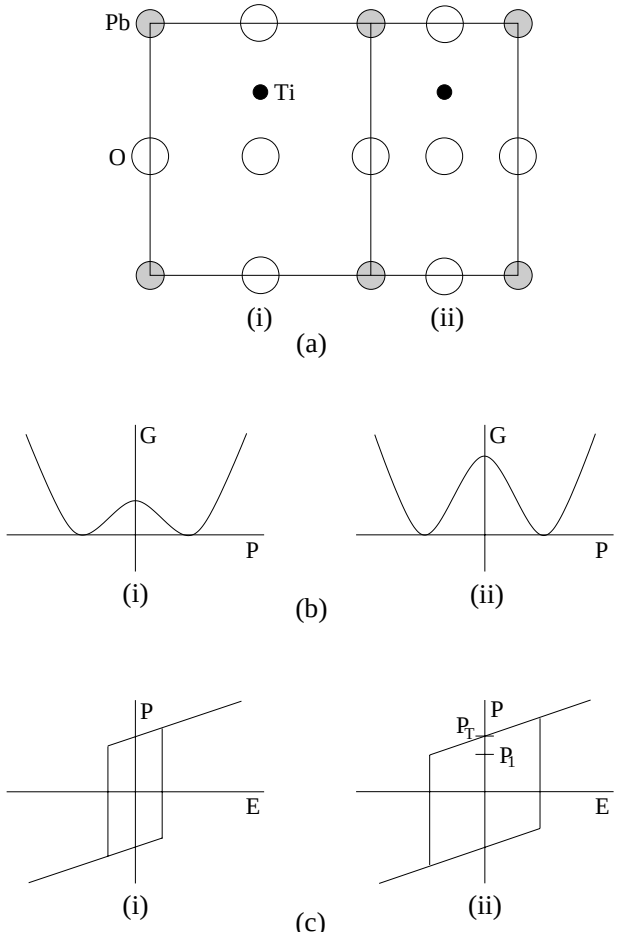

Figure 3. (a) Nonuniform lattice and polycrystalline structure for PZT; (b) Free energies associated with lattice widths (i) and (ii); (c) Variations in hysteresis kernel due to differing free energies.

single crystals with uniform lattices. In this initial model, we consider $\widetilde{E}_1$ to be normally distributed with mean $\bar{E}_1$. In this case, the total polarization is given by

$$P(E) = \int_0^\infty c_1 \overline{P}(E, \widetilde{E}_1) f(\widetilde{E}_1) d\widetilde{E}_1 \tag{9}$$

with the density

$$f(\widetilde{E}_1) = C_1 e^{-(\widetilde{E}_1 - \bar{E}_1)^2/b}, \tag{10}$$

and $\overline{P}$ is specified by (4). We note that in (9), the lower limit of 0 reflects the requirement that hysteresis kernels have nonnegative width. Alternatively f can be specified as a log-normal density to reflect the positivity of the kernel widths.

The second extension to the single crystal relation (4) is the consideration of effective fields in the material. As noted in [11, 13], the applied field in ferroelectric materials is augmented by fields generated by neighboring dipoles which produce nonhomogeneous effective fields in the materials. This produces variations about the applied field which can significantly alter the measured polarization. To incorporate these field variations, we consider the effective field to be normally distributed about the applied field. For fixed $\widetilde{E}_1$, the polarization in this case is given by

$$P(E) = \int_{-\infty}^\infty c_2 \overline{P}(\mathcal{E}) e^{-(E-\mathcal{E})^2/\bar{b}} d\mathcal{E} \tag{11}$$

where $\overline{P}$ is again specified by (4). The introduction of variations in the effective field produces domain switching in advance of the remanence point in accordance with observations from experimental data.

The complete polarization model combines the distributions defined in (9) and (11) to yield

$$[P(E,T)](t) = C \int_0^\infty \int_{-\infty}^\infty [\overline{P}(\mathcal{E}+E, \widetilde{E}_1, T)](t) e^{-\mathcal{E}^2/\bar{b}} e^{-(\widetilde{E}_1 - \bar{E}_1)^2/b} d\mathcal{E} d\widetilde{E}_1 \,. \tag{12}$$

We note that for implementation purposes, the infinite domains are truncated and the integrals are approximated using high-order Gaussian quadrature.

4. Model Validation

To illustrate the performance and prediction capabilities of the model, we consider the characterization of hysteresis and constitutive nonlinearities in a circular PZT5A wafer having a diameter of 2.54 cm (1 inch) and a thickness of $t = 0.0254$ cm (10 mils). The data was collected at 0.2 Hz for an input field having a maximum value of 2.36×10^6 V/m. We note that this field corresponds to a maximum input voltage of 600 V with the field and voltage related by the approximate expression $E = V/t$.

The parameters in the model were estimated through a least squares fit to the data with initial values of E_1 and P_T obtained from the asymptotic relations derived in Section 2. The least squares fit yielded the parameter values $E_1 = 40 \times 10^7, P_T = 0.033, \bar{E} = 1 \times 10^6, b = 1.5 \times 10^{11}, \bar{b} = 2 \times 10^4$ and $C = 1.44 \times 10^{-11}$.

The model prediction is compared with the experimental data in Figure 4. It is observed that the model accurately characterizes the observed hysteresis and saturation effects for this compound. Furthermore, with composite Gaussian quadrature routines used to approximate the integrals in (12), the algorithm is highly efficient to implement with full characterization requiring on the order of seconds on a workstation. This will facilitate the implementation of both optimization algorithms and inverse compensators which employ the model for control design.

5. Concluding Remarks

The theory presented in this paper combines free energy analysis at the microscopic level with stochastic averages to provide an efficient and accurate macroscopic model for characterizing hysteresis and constitutive nonlinearities in piezoceramic materials. It is also illustrated through examples in [14, 15] that this model

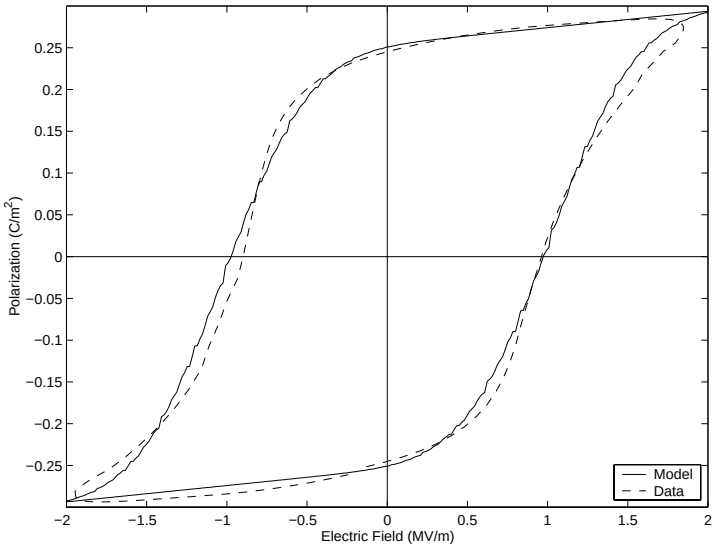

Figure 4. Model fit to 600 V PZT5A data from a circular wafer.

quantifies the quadratic Raleigh behavior observed at low drive levels and enforces closure of unbiased symmetric loops and biased asymmetric loops. This provides the model with extensive flexibility for a large number of operating regimes. Finally, the efficiency of the algorithm facilitates its incorporation in optimization routines for system design and inverse compensators for control design.

Acknowledgements

The research of R.C.S. was supported in part through the NASA grant NAG-1-01041 and in part by the Air Force Office of Scientific Research under the grant AFOSR-F49620-01-1-0107. The research of S.S. was supported in part by the National Science Foundation through the grant 0134464.

References

[1] W. Chen and C.S. Lynch, "A model for simulating polarization switching and AF-F phase changes in ferroelectric ceramics," *Journal of Intelligent Material Systems and Structures*, 9, pp. 427-431, 1998.

[2] W.S. Galinaitis and R.C. Rogers, "Compensation for hysteresis using bivariate Preisach Models," SPIE Smart Structures and Materials, 1997, Mathematics and Control in Smart Structures, San Diego, CA, 1997.

[3] P. Ge and M. Jouaneh, "Modeling hysteresis in piezoceramic actuators," *Precision Engineering*, 17, pp. 211-221, 1995.

[4] L. Huang and H.F. Tiersten, "An analytic description of slow hysteresis in polarized ferroelectric ceramic actuators," *Journal of Intelligent Material Systems and Structures*, 9, pp. 417-426, 1998.

[5] A.J. Moulson and J.M. Herbert, *Electroceramic: Materials, Properties, Applications*, Chapman and Hill, New York, 1990.

[6] R.E. Newnham, "Electroceramics," *Reports on Progress in Physics*, 52, pp. 123-156, 1989.

[7] M. Omura, H. Adachi and Y. Ishibashi, "Simulations of ferroelelectric characteristics using a one-dimensional lattice model," *Japanese Journal of Applied Physics*, 30(9B), pp. 2384-2387, 1991.

[8] N. Papenfuß and S. Seelecke, "Simulation and control of SMA Actuators," SPIE Smart Structures and Materials, Mathematics and Control in Smart Structures, San Diego, CA, pp. 586-595, 1999.

[9] G. Robert, D. Damjanovic and N. Setter, "Preisach modeling of piezoelectric nonlinearity in ferroelectric ceramics," *Journal of Applied Physics*, 89(9), pp. 5067-5074, 2001.

[10] S. Seelecke and C. Büskens, "Optimal control of beam structures by shape memory wires," *Computer Aided Optimum Design of Structures,* V.S. Hernández and C.A. Brebbia (Eds.,) Computational Mechanics Publications, pp. 457-466, 1997.

[11] R.C. Smith and C.L. Hom, "Domain wall theory for ferroelectric hysteresis," *Journal of Intelligent Material Systems and Structures*, 10(3), pp. 195-213, 1999.

[12] R.C. Smith and J.E. Massad, "A Unified Methodology for Modeling Hysteresis in Ferroic Materials," Proceedings of the 18th ASME Biennial Conference on Mechanical Vibration and Noise, to appear.

[13] R.C. Smith and Z. Ounaies, "A domain wall model for hysteresis in piezoelectric materials," *Journal of Intelligent Material Systems and Structures*, 11(1), pp. 62-79, 2000.

[14] R.C. Smith and S. Seelecke, "An energy formulation for Preisach models," Smart Structures and Materials 2002, Modeling, Signal Processing and Control in Smart Structures, to appear.

[15] R.C. Smith, S. Seelecke and Z. Ounaies, "A free energy model for ferroelectric materials," manuscript in preparation.